The Role of Deformation Banding in Grain Refinement under ECAP

Article *in* Materials Science Forum · May 2014

DOI: 10.4028/www.scientific.net/MSF.783-786.2641

4 authors, including:

Rustam Kaibyshev
Belgorod State University

S. S. Malopheyev
Belgorod State University

Marat Gazizov
Belgorod State University

Materials Science Forum Vols. 783-786 (2014) pp 2641-2646
© (2014) Trans Tech Publications, Switzerland
doi:10.4028/www.scientific.net/MSF.783-786.2641

The role of deformation banding in grain refinement under ECAP

Rustam Kaibyshev[1,a], Sergey Malopheyev[1,b], Vladislav Kulitskiy[1,c], Marat Gazizov[1,d]

[1]Laboratory of Mechanical Properties of Nanostructured Materials and Superalloys, Belgorod State University, Pobeda 85, Belgorod 308015, Russia

[a]rustam_kaibyshev@bsu.edu.ru, [b]malofeev@bsu.edu.ru, [c]kulitskiy@bsu.edu.ru, [d]gazizov@bsu.edu.ru,

Keywords: Aluminum alloys, Recrystallization, Dislocation structures, ECAP, Grain boundaries

Abstract. The mechanism of grain refinement in an Al-5.4Mg-0.4Mn-0.2Sc-0.09Zr alloy subjected to equal-channel angular pressing (ECAP) at 300°C through route B_C is considered. It was shown that the formation of geometrically necessary boundaries (GNB) aligned with a {111} plane at $\varepsilon \leq 1$ initiates the occurrence of continuous dynamic recrystallization (CDRX). Upon further strain the GNBs transform to low-to-moderate angle planar boundaries that produces lamellar structure. In the strain interval 2-4, 3D arrays of planar boundaries evolve due to inducing the formation of 2nd order and higher orders families of GNBs in new {111} planes. GNBs gradually convert to high-angle boundaries (HAB) with strain. A uniform recrystallized structure is produced at a true strain of ~8. The role of slip concentration and shearing patterns in the formation of GNBs is discussed.

Introduction

The grain refinement mechanisms operating during equal-channel angular pressing (ECAP) in aluminum alloys are still subject to debate [1-4]. Continuous dynamic recrystallization (CDRX) is the most probable mechanism providing grain refinement in aluminum alloys. In general, CDRX is a two-step phenomenon that includes the formation of stable three-dimensional (3D) arrays of deformation-induced low-angle boundaries (LABs) due to dislocation rearrangement followed by their gradual transformation into high-angle boundaries (HABs) [1,3]. The new grains form as a result of the increase in sub-boundary misorientation owing to continuous accumulation of the dislocations introduced by the deformation [1,3]. At intermediate temperatures, in aluminum alloys the formation of subgrains is the slowest process controlling the overall rate of the CDRX. The relatively high rate of CDRX under ECAP is attributed to the fact that the deformation banding results in the formation of planar geometrically necessary boundaries (GNBs) with moderate-to-high misorientation after first passes [1-5] that leads to the subdivision of the original grains into small, misoriented deformation bands [1,3]. It is apparent that this process plays a vital role in the formation of 3D networks of deformation-induced boundaries initiating CDRX [3]. However, to date, the relation between the deformation banding and grain refinement in ECAP processing is not completely understood.

The aim of this work is to consider the role of deformation banding in the grain refinement process occurring in the Al-Mg-Sc-Zr alloy, denoted as 1570C Al [6], and containing a dispersion of nanoscale coherent dispersoids, which suppresses the migration of deformation-induced boundaries. This alloy was subjected to ECAP with a back pressure (BP) using route B_C at an intermediate temperature of 300°C. At this temperature, the dislocation climb is operative [7] and may provide short-range rearrangement of lattice dislocations within dislocation boundaries [8], which leads to the easy formation of planar sub-boundaries. The application of a BP ensures that the mode of deformation occurs as a simple shear along the intersection plane.

Material and Experimental Procedures

The commercial 1570C Al with chemical composition of Al-5.4Mg-0.4Mn-0.2Sc-0.1Zr-0.3Ti (in weight %) was manufactured by semi-continuous casting and then subjected to solution treatment at

360°C for 8 hours and subsequent extrusion at an initial temperature of 380°C with ~50% reduction in cross section. The samples were machined from the central part of the extruded billet parallel to the extrusion direction into rods with a square cross-section of 20×20 mm^2. The channel had an L-shaped configuration with an angle of intersection of 90º. Deformation through this channel produced a strain of ~1 in each pass [1]. The sample was pressed under a pressure, P, and a constant back pressure, P_b = $0.2P_{max}$, that was applied using a back plunger in the exit channel [9]. The rods were pressed up to strains of ~1, ~2, ~4, ~6, ~8, and ~12 with a pressing speed of ~3 mm/s.

The specimens for microstructural examination were cut from the central parts of the pressed rods in the longitudinal direction parallel to the last pressing direction. Techniques of EBSD and TEM analysis were reported previously [9]. HABs and LABs were defined when adjacent pixels in the map have a misorientation of >15º and 2º<θ≤15º, respectively [1,9]. In addition, the statistics for LABs with misorientation 0.1º<θ≤2º were calculated within the remnant regions of unrecrystallized grains depicted as small squares on misorientation maps after hot extrusion and 1st, 2nd, 4th, and 6th ECAP passes. The misorientations on the LABs were additionally studied using a conventional Kikuchi-line technique [10].

Experimental results

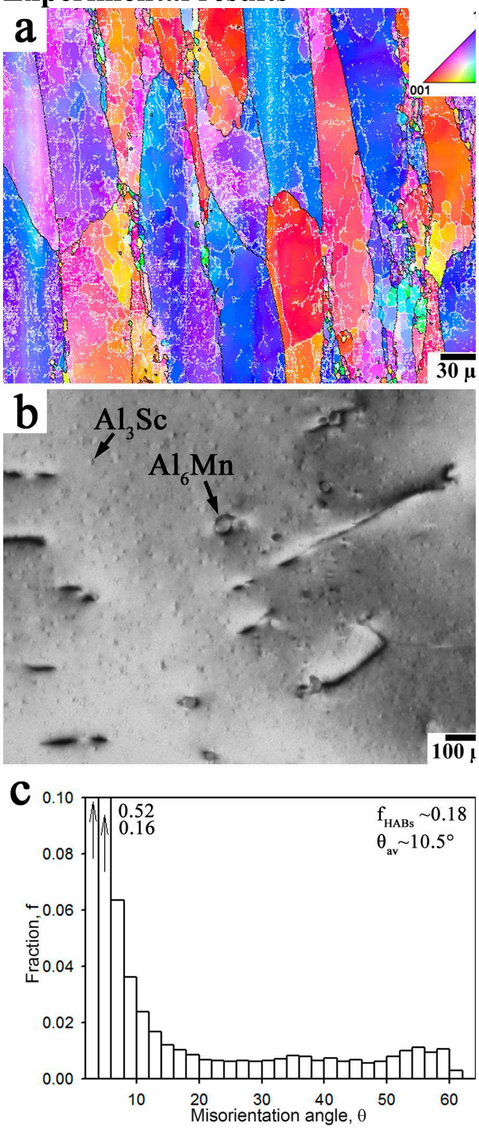

Figure 1. Initial microstructure after hot extrusion: (a) misorientation map, (b) TEM micrograph, (c) misorientation distribution.

Initial microstructure. The initial grains containing low dislocation density (ρ~10^{13} m^{-2}) were elongated along the extrusion direction (Fig. 1a); their average dimensions in the longitudinal and transverse directions were ~93 and ~30 μm, respectively. The fraction of HABs was ~18%, and the average misorientation was 10.5º (Fig. 1c). Two types of nanoscale dispersoids were observed. Coherent $Al_3(Sc,Zr)$ dispersoids having a size of ~10 nm were uniformly distributed, and round Al_6Mn-phase particles with an average size of ~38 nm were occasionally observed within the grains (Fig. 1b). The boundaries of these dispersoids with size ≥40 nm have an incoherent origin, and the interface boundaries of the dispersoids with size ≤20 nm are coherent or semi-coherent.

Deformation structure. The first ECAP pass introduces increased dislocation densities (ρ~4×10^{13} m^{-2}) and provides the formation of planar GNBs with average misorientation of ~4º (Fig. 2a). The alignment of all boundaries occurred at an angle of ~30º to the shear direction (Fig. 2a). Some planar boundaries have high-angle misorientation, which increased the fraction of HABs and the average misorientation to ~37% and 15º, respectively. The GNBs were identified as moderate-to-high planar boundaries which tend to be aligned with the most-stressed {111} slip plane with a small inclination angle [11] of approximately 15º (Fig. 3a). It is obvious that the {111} plane along which the GNBs evolve strongly deviates from the shear plane. In addition, planar GNBs evolve near original boundaries that results in the formation of directional ribbon grain structures (Fig. 2a). Next, these lamellas are subdivided by transverse LABs into sub-grains and/or (sub)grains bounded partly by LABs and partly by HABs (Fig. 2a). In the areas on unrecrystallized remnants of initial grains the formation of networks of LABs with average misorientation of ~0.5° takes place (Fig. 3a). Most of these sub-grains were essentially equiaxed in shape.

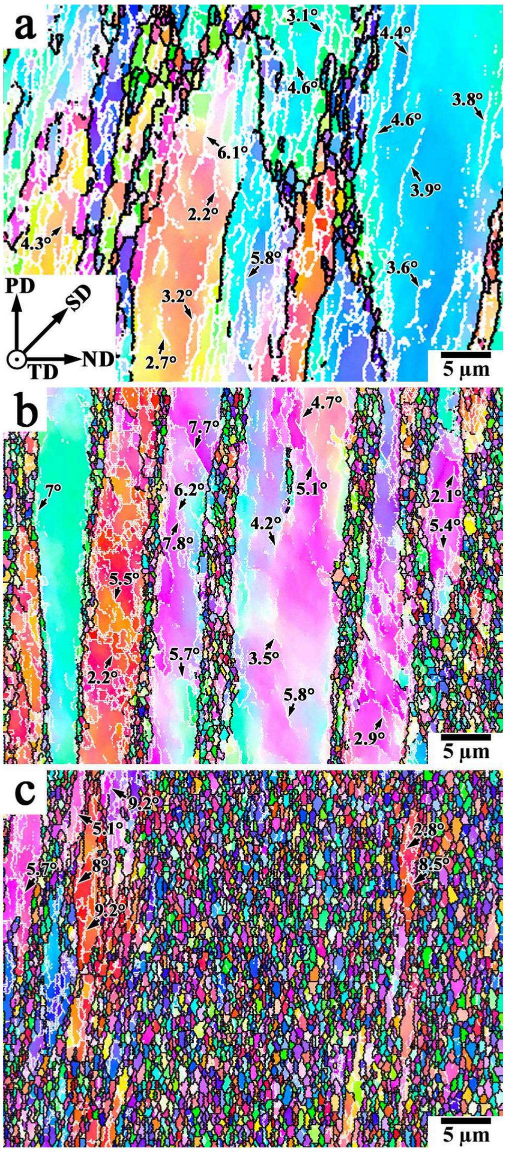

Figure 2. Typical OIM microstructures: (a) ε ~1, (b) ε ~4, (c) ε ~8.

Upon further deformation the chains of recrystallized grains formed along the initial boundaries, which were aligned at an inclination angle of ~40º to the shear direction, and the recrystallized volume fraction increases owing to thickening recrystallization bands (Fig. 2b,c). For ε~2, the density of the lattice dislocations within sub-grains was measured to be ~1.2×10^{14} m^{-2} and decreased insignificantly upon further strain. For ε~4, a partially recrystallized structure was observed (Fig. 3b). Recrystallized grains evolving on the original boundaries and lamellar structure near initial boundaries comprised the well-defined recrystallized bands (Fig. 2b). However, certain grain orientations are resistant to CDRX, and large remnants of initial grains remain (Fig. 2b). The formation of the new recrystallized layers occurred concurrently with increasing misorientation of the LABs, which delimited the deformation bands within the unrecrystallized region. As a result, the HAB fraction and the average misorientation tend to increase with strain. For ε~8, a fully recrystallized structure was observed (Fig. 2c). The grains contained a moderate density of lattice dislocations (ρ~6×10^{13} m^{-2}), and their boundaries were nearly free of grain boundary dislocations. The average sizes of the $Al_3(Sc,Zr)$ and Al_6Mn particles decreased slightly to ~9.7 nm and ~33 nm, respectively.

Three stages of CDXR during ECAP [1,3] are distinctly distinguished.

(i) For ε≤1, the values of θ_{av} (Fig. 4a) and V_{HAB} (Fig. 4b) increased to ~13° and ~28%, respectively. The dislocation density increased by a factor of 4.

(ii) For 1<ε≤2, a limited increase of the θ_{av} (Fig. 4a) and V_{HAB} (Fig. 4b) values with strain occurred, which led to a plateau of the values at ~13º and ~30 pct., respectively. The density of lattice dislocations increased by a factor of 2.5. The size of the grains and (sub)grains remained nearly unchanged.

(iii) In the strain interval from 2 to 8, the θ_{av} (Fig. 4a) and V_{HAB} (Fig. 4b) steeply increase with strain. The density of lattice dislocations remained essentially unchanged. The sizes of the grains and subgrains tended to increase with strain.

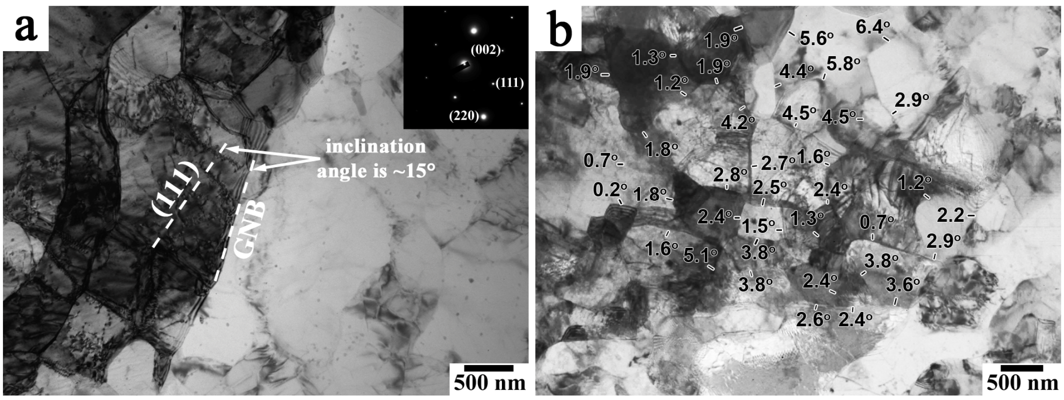

Figure 3. Typical TEM microstructures: (a) ε ~1 and (b) ε ~4.

A gradual transformation of LABs into HABs with strain led to the increasing volume fraction of the recrystallized grains. At ε>8, a slow increase and saturation of θ_{av} (Fig. 4a) and V_{HAB} (Fig. 4b) occurred because the recrystallized volume fraction attained ~70% for ε~8. Two main processes of microstructural evolution occurred within the central areas of original grains: first, transformation of LABs into HABs, and second, the subdivision of ribbon-like grains into (sub)grains of equiaxed shape. As a result, crystallites acquired essentially equiaxed shape with strain and the recrystallized volume fraction attained ~90% for ε~12.

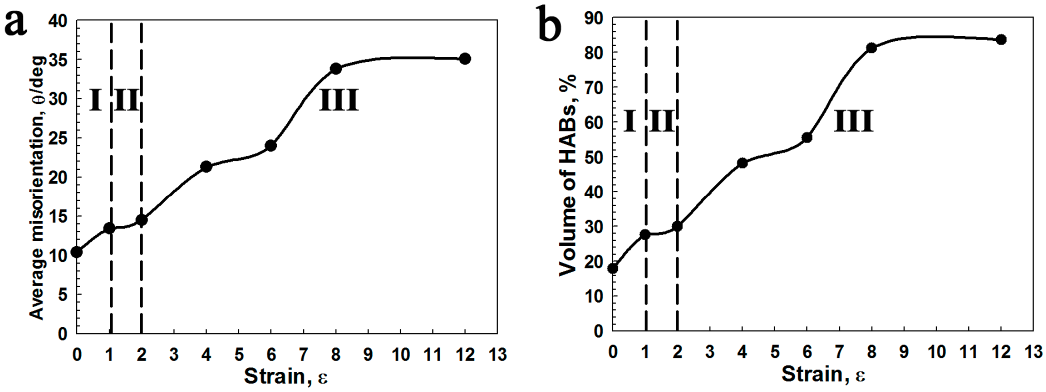

Figure 4. Effect of strain on (a) the average misorientation, θ; (b) the volume of HABs

Discussion

The extensive grain refinement in the 1570C Al during ECAP at intermediate temperatures is attributed to the initial formation of GNBs. The continuous lattice curvature is replaced by discrete boundary misorientations. In the present alloy the appearance of deformation-induced HABs is attributed solely to the formation of GNBs, and, therefore, the formation of GNBs plays a vital role in CDRX. ECAP promotes the rapid formation of the GNBs aligned with most stressed {111} planes [11] owing to high strain gradient within narrow zone of plastic deformation and the simple shear providing a very high-slip concentration in one {111} plane. One pass leads to a slip concentration in one {111} crystallographic plane, which tends to be aligned with the die-shearing plane. GNBs belonging to one family form. These boundaries easily transform into planar sub-boundaries due to the short-range rearrangement of the lattice dislocations by climbing within these boundaries. At ε~1, lamellas delimited by GNBs and original boundaries evolve. However, the formation of true grains entirely delimited by HABs requires the initial formation of 3D arrays of GNBs [1]. These 3D networks of deformation-induced boundaries can be produced in ECAP only by the subsequent activation of the dislocation glide in different {111} planes in consecutive passes due to the change in the shearing patterns from pass to pass occurring in such a way that provides the highest stress concentration in a new {111} plane in each consecutive pass. The route B_C provides the subsequent change of the most stressed planes belonging to {111} family from pass to pass. Rotation of the billet between first and second pressings provides the reorientation of planar subboundaries belonging to first family at an angle of ~120^o to the new shear plane. Extensive dislocation glide occurs along the other {111} plane, which is close to the die shearing plane (Fig. 5). In this case, the formation of the 2nd, and high-order families of GNBs occurs in the second, and subsequent passes, respectively, and the lamellar structure evolved after first pass is replaced by chains of recrystallized grains (Fig.3a-c) due to consecutive shearing of lamellas by new GNBs. The repetitive shearing eventually results in the development of crystallites entirely delimited by planar subboundaries which gradually transform to HABs with the high rate with strain.

CDRX during ECAP in the present alloy at intermediate temperatures is a three-step phenomenon. In stage I, the deformation banding introduces a large misorientation. The number of dislocations emitted by sources was significantly higher than the number of dislocations consumed for the formation of LABs with misorientation less than 2°. In Stage II, the formation of 3D networks of planar deformation-induced boundaries occurs. At this stage, the misorientation of GNB increases rapidly. However, the formation of 2nd order family of GNB, with an initially relatively low misorientation, provides an equilibrium balance between the increasing misorientations of GNB. In this stage, the ribbon structure eventually transforms into crystallites with an essentially round shape.

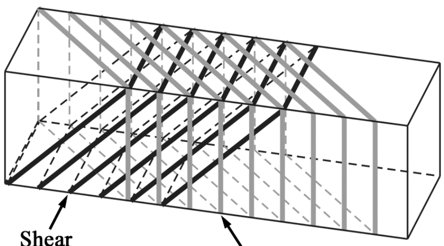

Figure 5. Schematic presentation of shearing pattern at 1st and 2nd passes

The formation of GNBs is accompanied by increasing density of lattice dislocations within the interiors of the deformation bands before a critical strain. It is apparent that the increases in the misorientation of deformation-induced boundaries and the density of these lattice dislocations occur concurrently in the lamellar structure continuously transforming to granular one, ε_c. In Stage III, the misorientations begin to increase rapidly beyond a critical strain, ε_c, due to the rapidly increasing misorientation of former GNBs delimiting individual domains, in which multiple slips occur. In this stage, the number of lattice dislocations accumulated by deformation-induced boundaries exceeds the number of dislocations stored within the interiors of the round crystallites. As a result, the density of lattice dislocations decreases slightly, and the rate of misorientation growth increases. In addition, in this stage, the orientations, which were initially resistant to CDRX, are reoriented and undergo recrystallization. Thus, the localized simple shear under ECAP is extremely important for the rapid evolution of 3D arrays of GNBs in aluminum alloys.

Conclusions

ECAP through route B_C is effective in extensive grain refinement in aluminum alloys because the simple shear provides a notably high-slip concentration in one {111} plane, which induces the formation of geometrically necessary boundaries aligned with this plane. After first pass the 1st family of geometrically necessary boundaries evolves, providing a rapid increase in the average misorientation, θ_{av}, and the portion of high-angle boundaries. After second and subsequent passes the 2nd and high order families of geometrically necessary boundaries evolves, which leads to the formation of a 3D network of planar boundaries. The ribbon-like structure is substituted by round crystallites. As a result, at a total strain ≥8, to the formation of a fully recrystallized structure with an average grain size of ~0.8 μm takes place.

Acknowlegement

Financial support from The Ministry of Education and Science of Russian Federation (project 14.A18.21.0760) is gratefully acknowledged. The authors also would like to thank a staff of Joint Research Center at Belgorod State University for technical assistance.

References

[1] R. Kaibyshev, K. Shipilova,F. Musin F, Y. Motohashi, Continuous dynamic recrystallization in an Al-Li-Mg-Sc alloy during equal-channel angular extrusion, Mater Sci Eng A 396 (2005) 341-351.

[2] Y. Huang, J.D. Robson, P.B. Prangnell, The formation of nanograin structures and accelerated room-temperature theta precipitation in a severely deformed Al-4 wt.% Cu alloy, Acta Mater 58 (2010) 1643-1657.

[3] I. Mazurina, T. Sakai, H. Miura, O. Sitdikov, R. Kaibyshev, Grain refinement in aluminum alloy 2219 during ECAP at 250 °C, Mater Sci Eng A 473 (2008) 297-305.

[4] Ch. Xu, M. Furukawa, Z. Horita, T.G. Langdon, The evolution of homogeneity and grain refinement during equal-channel angular pressing: A model for grain refinement in ECAP, Mater Sci Eng A 398 (2005) 66-76.

[5] D.A. Hughes, N. Hansen, D.J. Bammann, Geometrically necessary boundaries, incidental dislocation boundaries and geometrically necessary dislocations, Scr Mater 48 (2003) 147-153.
[6] R. Kaibyshev, E. Avtokratova, A. Apollonov, R. Davies, High strain rate superplasticity in an Al-Mg-Sc-Zr alloy subjected to simple thermomechanical processing, Scr Mater 54 (2006) 2119-2124.
[7] R. Kaibyshev, F. Musin, E. Avtokratova, Y. Motohashi, Deformation behavior of a modified 5083 aluminum alloy, Mater Sci Eng A 392 (2005) 373-379.
[8] A. Belyakov, T. Sakai, R. Kaibyshev, New grain formation during warm deformation of ferritic stainless steel, Metall Mater Trans 29 (1998) 161-167.
[9] A. Mogucheva, E. Babich, B. Ovsyannikov, R. Kaibyshev, Microstructural evolution in a 5024 aluminum alloy processed by ECAP with and without back pressure, Mater Sci Eng A 560 (2013) 178-192.
[10] P.B. Hirsch, A. Howie, R.B. Nicholson, D.W. Pashley, M.J. Whelan, Electron Microscopy of Thin Crystals, second ed., Krieger, New York, 1977.
[11] G. Winther, X. Huang, A. Godfrey, N. Hansen, Critical comparison of dislocation boundary alignment studied by TEM and EBSD: Technical issues and theoretical consequences, Acta Mater 52 (2004) 4437-4446.